EUROPEAN JOURNAL OF PURE AND APPLIED MATHEMATICS
2026, Vol. 19, Issue 1, Article Number 6760
ISSN 1307-5543 – ejpam.com
Published by New York Business Global

Numerical Analysis of Ceiling-Mounted Air Curtains for Reducing Airborne Pathogen Transmission in Offices

Mohamad Kanaan[1,*], Semaan Amine[2], Mohamed Hmadi[1]

[1] *Beirut Arab University, Faculty of Engineering, Mechanical Engineering Department, P.O. Box 11-5020, Riad El Solh, Beirut, 1107-2809, Lebanon*
[2] *College of Engineering and Technology, American University of the Middle East, Egaila 54200, Kuwait*

Abstract. Preventing airborne disease transmission in built environments is critically important for public health. This study employs computational fluid dynamics to evaluate the performance of ceiling-mounted air curtains in controlling the spread of airborne bacteria within an office space with dual conditioned zones. Multiple simulations were conducted, varying the air curtain's supply velocity while predicting the concentration of bacteria, in colony forming units per cubic meter, in the inhaled air of an exposed occupant to assess the system's effectiveness. Numerical results showed that, in a 2.8-m-high office, an air curtain ejection velocity of 1.5 m/s yielded optimal performance, improving the inhaled air quality by up to 96%. At lower velocities, the air curtain failed to effectively counteract pathogen diffusion, resulting in reduced protection. Conversely, excessively high velocities disrupted airflow patterns and compromised the separation between localized zones, thereby diminishing the curtain's effectiveness.

2020 Mathematics Subject Classifications: 76-04, 76-10

Key Words and Phrases: Air curtains, airborne pathogen transmission, computational fluid dynamics

1. Introduction

Indoor air quality (IAQ) is a global concern that affects individuals' health, comfort, and productivity. People spend over 87% of their time indoors, environments that are considered primary settings for the transmission of airborne illnesses [1]. Poor IAQ has been linked to a range of adverse health effects, including headaches, fatigue, difficulty concentrating, and irritation of the eyes, nose, and throat. It is also associated with the spread of respiratory illnesses caused by airborne bacteria, viruses, and fungi. In contrast, maintaining high IAQ promotes better health outcomes and enhances the productivity

*Corresponding author.
DOI: https://doi.org/10.29020/nybg.ejpam.v19i1.6760

Email addresses: m.kanaan@bau.edu.lb (M. Kanaan), semaan.amine@aum.edu.kw (S. Amine), m.hmadi@bau.edu.lb (M. Hmadi)

of occupants [2]. Heating, ventilation, and air conditioning (HVAC) systems function as the "respiratory system" of modern buildings, regulating indoor airflow, temperature, humidity, and air cleanliness. When these systems are poorly maintained or improperly operated, they can become sources of microbial contamination—compromising IAQ and posing serious health risks to occupants [3].

While HVAC systems play a critical role in maintaining IAQ and limiting the transmission of airborne contaminants through effective filtration and ventilation, they may not be entirely sufficient on their own. To enhance protection against pollutant infiltration, air curtains have emerged as a highly effective complement to HVAC systems. These devices generate a continuous stream of high-velocity air across open passages, forming an invisible barrier that blocks the intrusion of dust, fumes, and microorganisms—without restricting physical movement. By creating a "virtual partition," air curtains offer a non-invasive way to separate indoor spaces while preserving freedom of movement. This is particularly useful in shared offices, where unrestricted access between zones is needed. Kurec et al. [4] examined the utilization of an air curtain to mitigate the spread of virus-laden droplets from an infected individual to other passengers within a confined aircraft cabin. The findings indicate that the air curtain can effectively obstruct the transmission of small droplets (10–40 μm). Shih et al. [5] analyzed pollutant dispersion flow field using air curtains to improve emergency management crew safety in a polluted cleanroom after a large gaseous ethanol leak from a malfunctioning machine. By systematically changing ejection velocity, angle, and installation height, numerical simulations were performed to determine the importance of air curtains as a device which can control pollution and improve sealing.

Numerous computational fluid dynamics (CFD) studies demonstrated that air curtains effectively reduce the risk of infection and cross-contamination between distinct locations. Ye et al. [6] conducted a numerical investigation into the use of air curtains mounted on standard consulting desks to mitigate doctors' direct exposure to infectious exhaled contaminants. Simulation results revealed high effectiveness, with the average mass proportion of inhaled pollutants reduced by 70% to 90% in the consultation ward. Alanis et al. [7] utilized CFD and large eddy simulations to evaluate air curtain performance based on an adapted separation efficiency metric, defined by the rates of air infiltration and exfiltration across both sides of the air curtain barrier. Their findings demonstrate that separation efficiency is a versatile and robust performance indicator, applicable to a wide range of air curtain configurations—including downward, upward, and lateral blowing systems, as well as multi-jet setups. The metric effectively captures system behavior across diverse substances, transport mechanisms, and environmental conditions. He et al. [8] investigated the effectiveness of air curtain control in cleanrooms using CFD. Their results indicate that enlarging the air curtain's supply area can significantly lower pollutant concentrations within the cleanroom environment. Tan et al. [9] performed a numerical simulation using a Lagrangian particle tracking model to evaluate the performance of a ceiling-mounted air curtain in a surgical setting. The study found that increasing the air supply diffuser size from $4.32\,\mathrm{m}^2$ to $7.74\,\mathrm{m}^2$ resulted in a 33.3% reduction in particle count in the surgical zone.

While numerical models provide valuable insights, experimental studies are crucial

for validating air curtain effectiveness in real-world scenarios and optimizing their design to reduce cross-contamination in critical settings. In a full-scale isothermal experiment, Viegas et al. [10], explored strategies to limit contaminant migration between zones using air extraction from the "contaminated" compartment coupled with an air curtain. Their results indicated that the mean flow velocity across a doorway protected by an air curtain—necessary to maintain aerodynamic sealing—varies linearly with the Reynolds number. Huang et al. [11] investigated the aerodynamic behavior and containment performance of a biological safety cabinet equipped with an air curtain at the front opening, using laser-based visualization and tracer gas concentration detection techniques. The system employs a thin, flat jet emitted from the bottom edge of the sash, coupled with a suction flow through a slot located at the front edge of the work surface—together forming an air curtain across the cabinet opening. In the "slightly concave" curtain configuration, the flow pattern remained smooth and two-dimensional, effectively separating the cabinet interior from the external environment. This configuration demonstrated minimal containment escape, inward dispersion, and cross-cabinet contamination.

Although considerable research has explored the role of air curtains in regulating IAQ, no previous studies have addressed their performance in office spaces featuring two distinct localized zones, each equipped with dedicated supply and exhaust grills. This represents a notable gap in understanding their effectiveness in mitigating airborne disease transmission in such environments. Moreover, the existing air curtain literature lacks numerical investigations that quantify airborne bacteria concentration using colony-forming units (CFU) per cubic meter, the standard metric that facilitates practical relevance and real-world applicability. This paper aims to bridge these gaps by evaluating the performance of a ceiling-mounted air curtain in an office setting occupied by both a healthy and an infected individual, each situated within a separately ventilated zone. Specifically, it examines how optimizing the air curtain's supply velocity can enhance protection for the exposed occupant.

2. Methods

2.1. System description

The study examines an office space located in Beirut, measuring $5.20 \times 2.72 \times 2.80$ meters (Figure 1). It contains two workstations, each occupied by a seated individual generating a heat output of 1 Met (58.15 W/m^2), representative of a sedentary adult [12], alongside a 65 W computer. For simplicity, each occupant is modeled using a block-shaped person simulator, an approach commonly employed in existing literature [13, 14]. The office features north- and west-facing exterior walls, while the remaining walls and the floor are treated as internal partitions. Uniform ceiling-mounted lighting provides a typical luminous flux of 11.8 W/m^2 across the space [15].

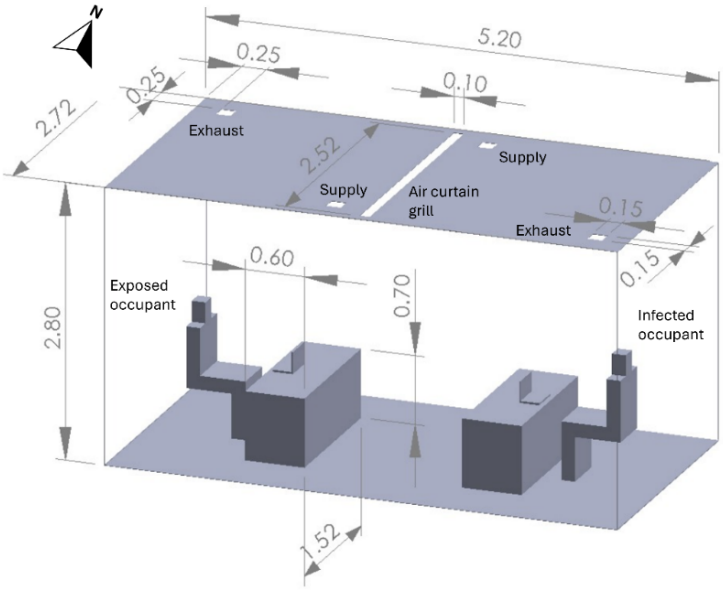

Figure 1: Schematic of the simulated office.

Each occupant exhales at a rate of 8.4 L/min [16] through a circular mouth opening, with an airflow velocity of 1 m/s and a temperature of 34°C [17]. These conditions reflect typical breathing and speaking patterns consistent with office-related activities. One of the occupants is infected and emits approximately 50 CFU/s of bacteria by breathing and talking. The other individual, assumed to be healthy, is referred to as the exposed occupant.

A ceiling-mounted linear grill, measuring 2.7 × 0.1 m^2, delivers a 24°C air curtain that separates the two workstations, effectively dividing the room into two zones of equal volume. Each zone is equipped with a supply diffuser and an exhaust diffuser, both measuring 0.15 × 0.15 m^2. Conditioned air at 14°C is delivered through each supply grill at a rate of 36 L/s. The curtain temperature was set to 24°C, aligning with the indoor setpoint to prevent any adverse effects on thermal comfort. Additionally, lowering the temperature below 24°C would lead to increased energy consumption by the cooling system.

2.2. Numerical modelling

A comprehensive three-dimensional computational fluid dynamic (CFD) model was developed to simulate the office space. CFD is a scientific discipline focused on numerically solving the non-linear partial differential equations that govern fluid motion and heat transfer, primarily the Navier–Stokes and energy equations. In this study, simulations were conducted using the commercial CFD software ANSYS Fluent v.15.3, which employs an implicit finite volume method with iterative solvers to ensure stability and accuracy

in resolving complex flow fields. The study then presents numerical predictions that have not been experimentally validated. However, numerous studies have concluded that the application of CFD to indoor airflow simulation has yielded significant success [18–20]. Furthermore, the use of a high-quality computational mesh, well-defined boundary conditions, carefully chosen solution methods, grid-independence analysis, and stringent convergence criteria collectively contribute to the reasonable reliability of the results [21]. The simulated domain was discretized using tetrahedral finite volumes, resulting in a computational grid with skewness values maintained below 0.9 to ensure mesh quality. Three mesh sizes were evaluated—532,455 cells, 950,812 cells, and 1,290,691 cells. The dependence of the quantities of interest on the cell count is detailed in Table 1.

Table 1: Results of the grid independence analysis

Mesh	**No. of cells**	**Velocity diff. (%)**	**Temperature diff. (%)**
Mesh 1	532,455	–	–
Mesh 2	950,812	12.7	5.8
Mesh 3	1,290,691	3.8	1.1

The results demonstrated that the 950,812-cell mesh, shown in Figure 2, achieved grid-independent solutions and was subsequently adopted for all simulation cases. The mesh featured a minimum element size of 9 mm and a maximum of 72 mm, with targeted refinements applied near openings to accurately capture high-gradient regions.

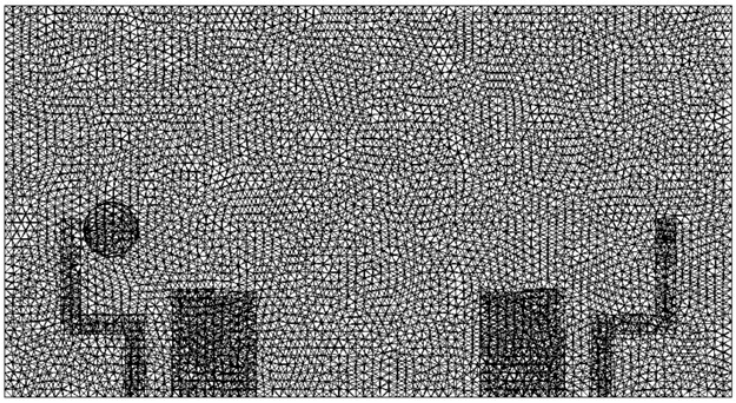

Figure 2: Computational grid used in the simulations.

Indoor airflow was simulated using the Realizable k–ε turbulence model, under the assumptions of steady-state and incompressible flow. This model is well known for its reliability in predicting indoor air flows [22, 23]. Buoyancy effects were incorporated using the incompressible ideal gas model, which accounts for temperature-induced density variations. To capture thermal radiation, the surface-to-surface (S2S) radiation model was employed, assuming surfaces to be grey and diffuse. The governing transport equations, presented in their general form in Equation (1), were numerically solved using the CFD

solver.

$$\nabla \cdot (\rho \mathbf{v}\, \phi) = \nabla \cdot (\Gamma_\phi \nabla \phi) + S_\phi \tag{1}$$

where v represents the velocity field, ϕ denotes the transported scalar variable, Γ_ϕ is the effective diffusivity, and S_ϕ is the corresponding source term. This study investigates the airborne transmission of disease through droplet nuclei, dried residues of small expiratory droplets that can remain suspended in the air for prolonged periods. Typically measuring between 1 and 5 μm in diameter, these particles serve as a primary vector for the spread of numerous infectious diseases via the airborne route. In contrast, larger expiratory droplets tend to settle rapidly due to gravity, depositing onto surfaces and thereby contributing to the contact-based mode of transmission. Therefore, the species transport model was employed to estimate airborne bacterial concentration fields within the simulated office. The concentration of bacterial droplet nuclei was treated as a passive scalar, fully governed by the underlying airflow dynamics, and interpreted as the number of airborne bacteria per cubic meter of air, typically expressed in CFU. Considering the variability in bacterial types, sizes, and the impact of drying on bacterial viability, a simplified assumption was adopted: droplet nuclei with a diameter of 1 μm were modeled, each assumed to carry a single bacterium. Furthermore, a conservative approach was taken by assuming that each viable bacterium gives rise to a single colony [24].

A second-order UPWIND scheme was employed to discretize the air-related variables, while pressure was discretized using the STANDARD scheme. Velocity and pressure coupling in the Navier–Stokes equations was achieved using the SIMPLE algorithm. Convergence of the numerical solution was assumed when the scaled residuals dropped to the magnitude of 10^{-5}, and the bacterial concentration within the respiration zone reached a stable value.

Simulations were conducted across a range of air curtain supply velocities. The scenario without an air curtain, representing the office environment, served as the baseline case for comparison. For each simulation, the effectiveness of the air curtain was evaluated using the predicted concentration of bacterial droplet nuclei in the respiration zone of the exposed occupant, based on the following equation:

$$\eta \;=\; 1 - \frac{C_i, with\, curtain}{C_i, without\, curtain}, \tag{2}$$

where C_i denotes the volume-average concentration of bacterial droplet nuclei in the inhaled air, specifically within the occupant's respiration zone. This zone was defined during the simulation's pre-processing stage as a sphere of influence with a diameter of 40 cm, located 2.5 cm from the occupant's nose [25], as illustrated in Figure 3.

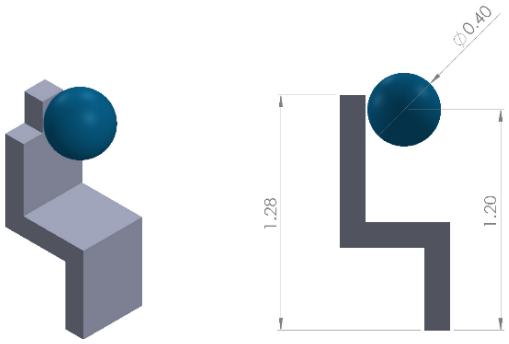

Figure 3: Respiration zone of the exposed occupant.

The boundary conditions applied in the simulations are summarized in Table 2. A velocity inlet boundary condition was applied to the supply diffusers and the air curtain grill, as the flow scalar properties, namely velocity and temperature, were predefined prior to the simulation. Heat gains through exposed walls were estimated using DesignBuilder software, based on cooling season design conditions specific to Beirut.

Table 2: Boundary conditions for the simulations

Boundary	**Type**	**Details**
Supply diffuser	Velocity inlet	$T = 14°C$; $V = 1.6\,m/s$; $I = 10\%$ [26]; hydraulic diameter $= 0.15\,m$
Exhaust diffuser	Pressure outlet	Default values
Air curtain grill	Velocity inlet	$T = 24°C$; $V = 1, 1.25, 1.5, 1.75, 2\,m/s$; $I = 10\%$; hydraulic diameter $= 0.192\,m$
Person simulator	No slip	Heat flux $= 58.15\,W/m^2$
Infected mouth	Velocity inlet	$T = 34°C$; $V = 1\,m/s$; $I = 5\%$; $D_h = 0.0134\,m$; bacterial droplet nuclei molar fraction $= 1.8 \times 10^{-13}$
Ceiling	No slip	Heat flux $= 11.8\,W/m^2$
Floor/partitions	No slip	Zero heat flux
Exterior walls	No slip	Heat flux $= 6.8\,W/m^2$ (north), $15.6\,W/m^2$ (west)

3. Results and discussion

The airflow patterns and bacterial droplet nuclei distributions on a symmetry plane for the baseline case are shown in Figure 4, while the CFD plots for the air curtain simulated cases are shown in Figure 5.

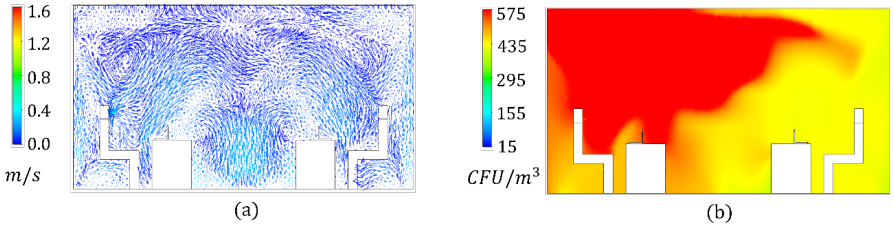

Figure 4: CFD plots of (a) air velocity and (b) pathogen concentration distributions without the use of air curtain.

In the absence of an air curtain, the airflow demonstrates complete mixing throughout the office space, resulting in high exposure to bacterial spread for the occupant. This transmission occurs through both convection and diffusion. In contrast, when an air curtain is present, the space divides into two distinct mixed zones. The descending flow from the air curtain acts as a barrier, and its effectiveness increases with higher supply velocity. As the curtain's momentum strengthens, it more effectively prevents airborne contaminants from crossing into the exposed occupant's localized zone, thereby offering enhanced protection. However, at excessively high supply velocities (cases d and e), the curtain impinges on the floor and rebounds upward, disrupting the intended separation. This backflow facilitates the transport of pathogenic droplet nuclei into the occupant's respiration zone, thereby compromising the quality of inhaled air, a result consistent with the findings reported in [6].

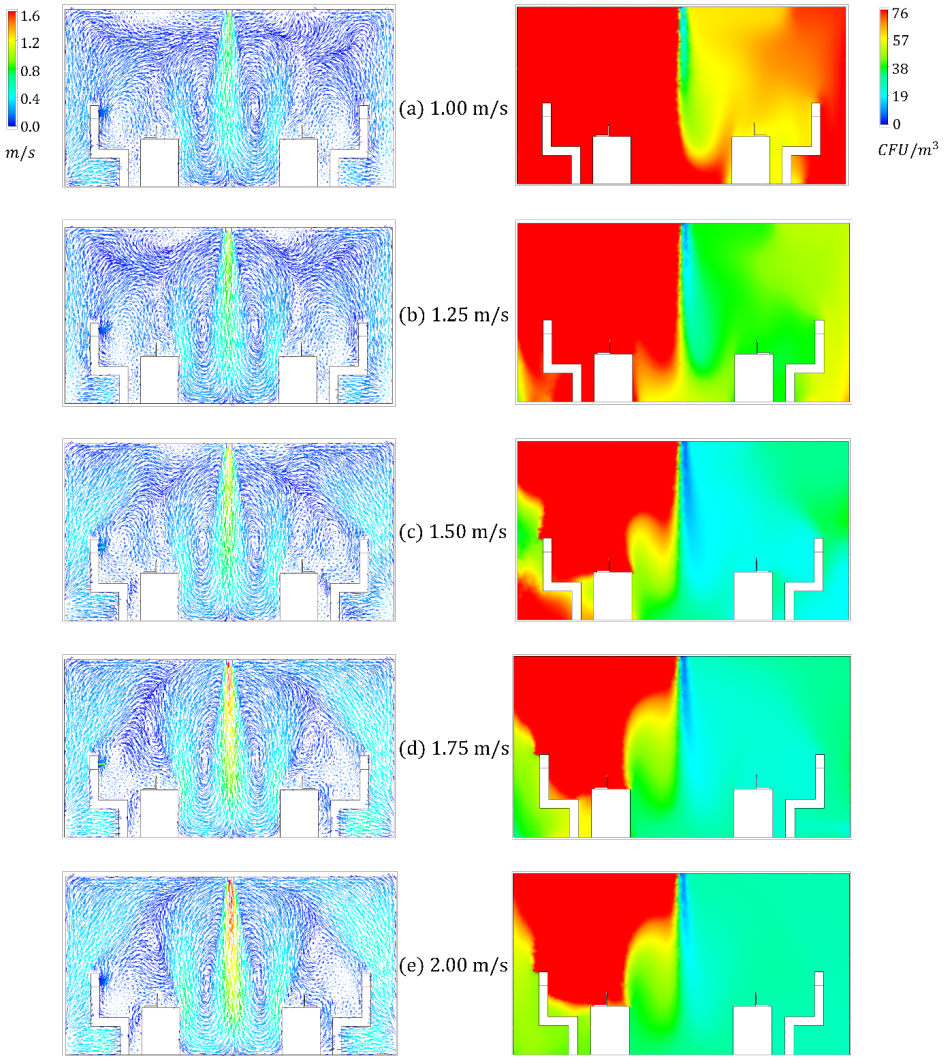

Figure 5: CFD plots for different air curtain ejection velocities.

Table 3 presents the predicted concentrations within the respiration zone of the exposed occupant and the corresponding effectiveness of the air curtain in mitigating airborne disease transmission across all simulated scenarios.

Table 3: CFD predictions of bacteria concentration in the exposed occupant's inhaled air and corresponding air curtain effectiveness

Case	**Bacteria conc. (CFU/m^3)**	**Air curtain effectiveness**
Baseline – no curtain	431	–
1.00 m/s	61	0.86
1.25 m/s	40	0.91
1.50 m/s	17	0.96
1.75 m/s	24	0.94
2.00 m/s	30	0.93

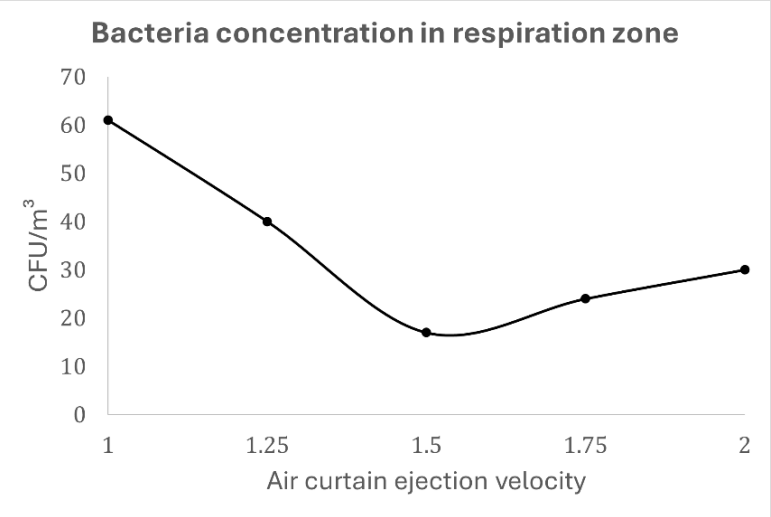

Figure 6: Variations of bacteria concentration in the exposed occupant's inhaled air with air curtain supply velocity.

4. Conclusion

A detailed three-dimensional CFD model was developed to simulate the airflow within an office environment featuring a standard ceiling height of 2.8 meters. The space is occupied by one infected and one uninfected individual, allowing for the analysis of potential airborne transmission. The office is divided into two identical localized zones, each equipped with dedicated supply and exhaust grilles as components of a mixed-mode ventilation system. A centrally positioned, ceiling-mounted air curtain separates the two zones, serving as a barrier to limit cross-contamination between the two occupants. The model predicted the concentration of pathogenic droplet nuclei within the respiration zone of the exposed occupant, enabling assessment of the air curtain's effectiveness in mitigating airborne pathogen transmission under varying ejection velocities. Simulation results indicated that an optimal ejection velocity of 1.5 m/s provided maximum protection, reducing exposure by up to 96%. Lower velocities offered diminished protection, while higher velocities compromised effectiveness due to flow disturbances caused by air backflow after impacting the floor. Although the parameters and boundary conditions employed in this study align with typical office environments, further investigation is warranted to better evaluate the effectiveness of air curtains in mitigating airborne disease transmission under a broader spectrum of conditions, including varying ceiling heights, ejection angles, exhaled flow rates, and human heat flux densities. The intricate interactions between exhaled airflow and air curtain dynamics may influence the dispersion and containment of airborne contaminants.

References

[1] M. Cheng, B. Kong, C. Song, Y. Li, and H. Shi. Optimization of cabin virus transmission suppression technology based on hanging curtain physical isolation. *Applied Sciences*, 14:2948, 2024.

[2] J. Wei and Y. Li. Airborne spread of infectious agents in the indoor environment. *American Journal of Infection Control*, 44:S102–S108, 2016.

[3] Z. Liu, S. Ma, G. Cao, C. Meng, and B. J. He. Distribution characteristics, growth, reproduction and transmission modes and control strategies for microbial contamination in hvac systems: A literature review. *Energy and Buildings*, 177, 2018.

[4] K. Kurec, B. Olszański, K. Gumowski, M. Klamka, M. Remer, J. Piechna, and S. Kubacki. Air curtain as a sars-cov-2 spreading mitigation method in a small aircraft cabin. *Proc Inst Mech Eng G J Aerosp Eng*, 237, 2023.

[5] Y. C. Shih, A. S. Yang, and C. W. Lu. Using air curtain to control pollutant spreading for emergency management in a cleanroom. *Building and Environment*, 46, 2011.

[6] J. Ye, H. Qian, J. Ma, R. Zhou, and X. Zheng. Using air curtains to reduce short-range infection risk in consulting ward: A numerical investigation. *Building Simulation*, 14, 2021.

[7] C. Alanis Ruiz, T. van Hooff, B. Blocken, and G. van Heijst. Air curtain performance:

Introducing the adapted separation efficiency. *Building and Environment*, 188:107468, 2021.

[8] J. He, H. Xu, M. Cao, Q. Liang, S. Zhang, M. Yu, H. Liu, Z. Liu, and J. Liu. Assessment of air curtain control efficacy in preventing contaminant transmission in cleanrooms. *Indoor Air*, 2025.

[9] H. Tan, K. Y. Wong, C. T. Lee, S. L. Wong, B. B. Nyakuma, R. A. Wahab, K. Q. Lee, M. C. Chiong, W. S. Ho, M. H. D. Othman, Y. H. Yau, H. Y. Kek, and H. M. Kamar. Numerical assessment of ceiling-mounted air curtain on the particle distribution in surgical zone. *Journal of Thermal Analysis and Calorimetry*, 148, 2023.

[10] J. C. G. Viegas, L. Carrasco, L. Pinto, J. Morais, P. Morais, and D. Aelenei. Full-size experimental assessment of the aerodynamic sealing of low velocity air curtains. *Fluids*, 6:359, 2021.

[11] R. F. Huang and C. I. Chou. Flow and performance of an air-curtain biological safety cabinet. *Annals of Occupational Hygiene*, 53, 2009.

[12] P. O. Fanger. *Thermal Comfort*. McGraw-Hill, New York, 1972.

[13] A. Asral, R. Abdurrahman, W. C. Khoo, I. Taib, N. A. H. Roseman, K. H. Kong, C. S. Lee, K. S. Jesni, and A. Martin. Cfd analysis of coronavirus dispersion through breathing in aircraft cabin environments. *Journal of Advances in Fluid, Heat, and Materials Engineering*, 1:49–59, 2025.

[14] M. Kanaan, S. Amine, and E. Gazo-Hanna. Optimizing supply conditions and use of return air in ufad system: Assessment of iaq, thermal comfort and energy performance. *Results in Engineering*, 24:103426, 2024.

[15] R. Singh and R. Rawal. Effect of surface reflectance on lighting efficiency in interiors. In *Building Simulation 2011: 12th Conference of International Building Performance Simulation Association (IBPSA)*, pages 2301–2308, Sydney, 2011.

[16] C. Habchi, K. Ghali, N. Ghaddar, W. Chakroun, and S. Alotaibi. Ceiling personalized ventilation combined with desk fans for reduced direct and indirect cross-contamination and efficient use of office space. *Energy Conversion and Management*, 111:158–173, 2016.

[17] F. Liu, L. Zhang, and H. Qian. The penetration phenomenon of the expiratory airflow from thermal plume of human body in the microenvironment around people. *Building and Environment*, 259:111656, 2024.

[18] S. Alimi, R. Nciri, F. Nasri, Y. A. Rothan, and C. Ali. Performance investigation of an original hybrid solar façade system used for hdh desalination and building natural ventilation. *Journal of Building Engineering*, 42:102515, 2021.

[19] A. Askari, M. Mahdavinejad, and M. Ansari. Investigation of displacement ventilation performance under various room configurations using computational fluid dynamics simulation. *Building Services Engineering Research and Technology*, 43:627–643, 2022.

[20] F. Nasri. Numerical simulation of a efficient solar-powered ventilation system. *Engineering, Technology & Applied Science Research*, 13:11459–11465, 2023.

[21] Y. Li and P. V. Nielsen. Cfd and ventilation research. *Indoor Air*, 21:442–453, 2011.

[22] S. A. Nada, H. M. El-Batsh, H. F. Elattar, and N. M. Ali. Cfd investigation of airflow pattern, temperature distribution and thermal comfort of ufad system for

theater buildings applications. *Journal of Building Engineering*, 6:274–300, 2016.

[23] A. Patel, B. Saikiran, G. N. Suraj, R. Kumar, S. W. A. Chisty, G. A. Ganesh, and S. L. Sinha. Numerical analysis of naturally ventilated indoor environment for different turbulence models. In *AIP Conference Proceedings*, page 080023, 2023.

[24] M. Kanaan, N. Ghaddar, K. Ghali, and G. Araj. New airborne pathogen transport model for upper-room uvgi spaces conditioned by chilled ceiling and mixed displacement ventilation: Enhancing air quality and energy performance. *Energy Conversion and Management*, 85:50–61, 2014.

[25] J. Karam, K. Ghali, and N. Ghaddar. Resilience of personalized ventilation in maintaining acceptable breathable air quality when combined with mixing ventilation subject to external shocks. *Buildings*, 14:654, 2024.

[26] D. Y. Park and S. Chang. Numerical investigation of thermal comfort and transport of expiratory contaminants in a ventilated office with an air curtain system. *Indoor and Built Environment*, 28:401–421, 2019.